Proceedings of 20th International Congress on Acoustics, ICA 2010

23-27 August 2010, Sydney, Australia

A High Power Piezoelectric Ultrasonic Linear Micromotor Using Slotted Stator

Cheol-Ho Yun (1), Brett Watson (1), James Friend (1) and Leslie Yeo (1)

(1) Micro/Nanophysics Research Laboratory, Department of Mechanical Engineering,

Monash University, Clayton, Victoria, Australia

PACS: Type 43.38.Fx Piezoelectric and ferroelectric transducers

ABSTRACT

A novel ultrasonic micro linear motor that uses 1st longitudinal and 2nd bending modes, derived from bar type stator with a rectangular slot cut through the stator length, has been proposed and designed for end-effect devices of micro-robotics and bio-medical applications. The slot structure plays an important role in the motor design, and can be used not only to tune the resonance frequency of the two vibration modes but also to reduce the undesirable longitudinal coupling displacement due to bending vibration at the end of the stator. By using finite element analysis, the optimal slot dimension in order to improve the driving tip motion was determined, resulting in the improvement of the motor performance. The trial linear motor, with a weight of 1.6g, gave a maximum driving velocity of 1.12 m/s and a maximum driving force of 3.4 N. A maximum mechanical output power of 1.1 W was obtained at force of 1.63 N and velocity of 0.68 m/s. The output mechanical power per unit weight was 688 W/kg.

INTRODUCTION

Ultrasonics and piezoelectric motors can be an attractive alternative to electromagnetic motors for end-effect devices such as microbot joints [1], bio-medical and mobile device applications [2], due to their small size, compact structure, light weight and high mechanical output.

For linear drive applications, many types of ultrasonic linear motors (USLM) have been developed. Among various kinds of ultrasonic linear motors, the bimodal ultrasonic linear motors using first longitudinal and second bending mode (L1B2) are well known motors and can be driven with higher output and higher precision positioning [3]. Based on the construction method, USLMs can be classified into bolt-clamped Langevin transducer (BLT) type [3], [4], rectangular piezoelectric plate type [5]-[8] and bonded metal/piezo-ceramic type [9] motors.

A BLT type USLM associated with the piezoelectric d_{33} coefficients has been successfully developed with an output force of 100 N. However, a coupling problem due to the longitudinal motion associated with the bending mode, potentially degraded the performance of the motor [4]. This coupling problem was improved by adopting a much longer length stator [3]. However, the construction method of this BLT motor was to use several thickness-poled Lead Zirconate Titanate (PZT) disks sandwiched by metal blocks with a bolt. This method is complex and makes assembly and size reduction difficult.

Alternatively, rectangular piezoelectric plate type and bonded metal/piezo-ceramic type USLMs using in-plane vibrations with piezoelectric d_{31} coefficients can be constructed simply and, at small scales. A well-known design is bimodal plate USLM developed by *Nanomotion* [5]. This motor has one driving tip placed at one end of the stator, which transfer cyclic vibratory motion to a slider pressed against it. Other rectangular plate type USLMs with two driving tips have been developed [6], [9], which are a very attractive arrangement to save mounting space. These motors are similar to that of the design of *Nanomotion*, with the exception that the piezoelectric plate is arranged lengthwise with two attached driving tips on the same length side. Two driving tips are attached to the positions of relatively higher bending displacement but not the highest longitudinal displacement position, avoiding the coupling problem of bending vibration. However, such arrangement will prevent the maximum motor performance being achieved.

In this paper, a novel ultrasonic linear micromotor using the 1st longitudinal and 2nd bending modes of a slotted structure is proposed. This slot structure plays an important role in motor design, which can tune the two vibration modes with same resonance frequency and decrease the undesirable longitudinal coupling displacement due to bending vibration at the end of the stator.

CONSTRUCTION AND OPERATING PRINCIPLE

The configuration of the slotted bar type vibrator stator for a new micro ultrasonic linear motor is shown in Fig. 1. The stator consists of two PZT (C-213, Fuji Ceramic Co., Japan) elements and a titanium (Ti-6Al-4V, Ti64) metal bar, with a rectangular slot cut through the bar length (machined using a computer-controlled micro-electro discharge machining process, micro-EDM). The two PZT elements are bonded to

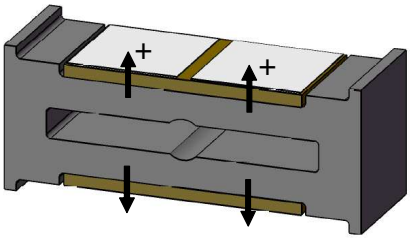

(a)

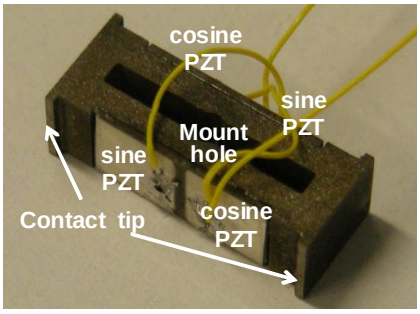

(b)

Figure 1. The configuration of the slotted bar type stator: (a) CAD model, and (b) photos of a prototype.

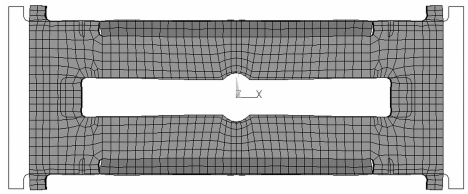

(a)

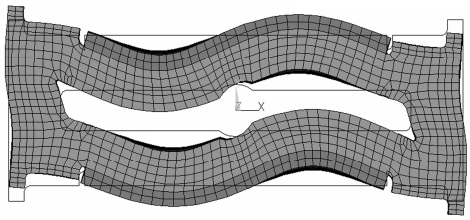

(b)

Figure 2. Vibration modes of the stator: (a) 1st longitudinal mode and (b) 2nd bending mode.

the two opposite flattened sides of the metal component using an epoxy. Each PZT element has one side divided into two top electrodes with same poling directions and a uniformly formed bottom electrode which is connected to the ground. The PZT plates were polarized in the thickness directions and directions are indicated by the thick arrows in Fig. 1(a). The stator has four signal input electrodes, which are connected in diagonal pairs, to excite the vibrations. One pair of electrodes is excited as a sine input and the other pair is excited as a cosine input, as shown in Fig. 1(c). To prevent vibration distortion due to the shape imbalance of the stator, four tips (for frictional components) were positioned symmetrically at the stator ends and formed in one body with the stator. When the two pairs of electrodes are operated with same phase and resonance frequency, the first longitudinal (L1) mode is generated and the tips of stator have a horizontal displacement component (Fig. 2(a)). With anti-phase operation of the

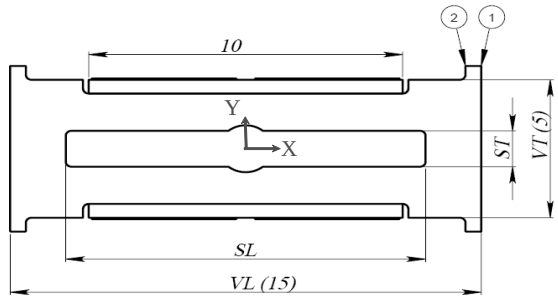

Figure 3. The model stator and parameters for FEA.

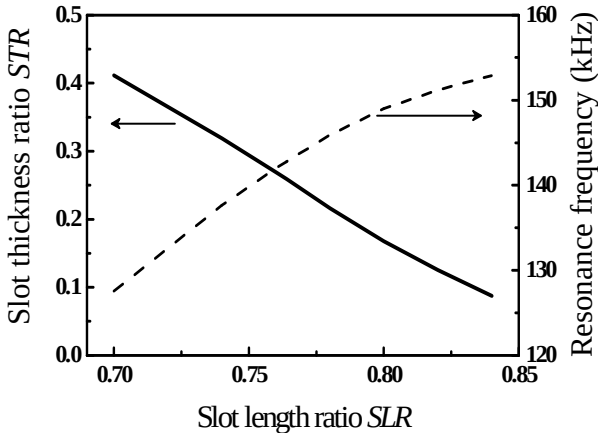

Figure 4. The modal analysis simulation results for the effect of changing the slot dimension.

electrode pairs, the stator tips vibrate with vertical displacement resulting from the second bending (B2) mode (Fig. 2(b)). By applying the two electrical sine waves to the two electrode pairs with a temporal 90 degree phase difference, the two vibration modes are excited simultaneously with phase difference of 90 degrees. As a result, an elliptical motion is excited at the tips of the stator, which drives the slider through friction force between tip and slider [4]. Note the locus at one end of stator is delayed by 180 degrees compared to that of the other end. Therefore, one of the two ends is contacting and driving the slider with anti-phase. By changing the driving phase between the two electrode pairs, the elliptical motion of the tips changes direction, resulting in a reversed of the slider direction.

DESIGN OF THE STATOR

The trial motor has a simple structure and modes, but the driving tips of stator have a complicated vibration motion. As such, a simple analytic analysis is inadequate for design. A finite element analysis (FEA) program ANSYS (ANSYS Inc., USA) was used to conduct the modal and harmonic analysis of the stator and to predict the slot effect for the tip vibration motion. The FEM analysis was carried out without the bonding layer between the PZT and metal body due to the increased complication of such a model. The geometric boundary condition of the model was a free-free case. The nodes along the faces of the PZT element were merged to the electrode, which is described in detail elsewhere [10]. The model employed a complete model of hard PZT (c-213, Fuji Ceramic, Japan), incorporating an anisotropic electric permittivity, piezoelectric stress coupling, and stiffness.

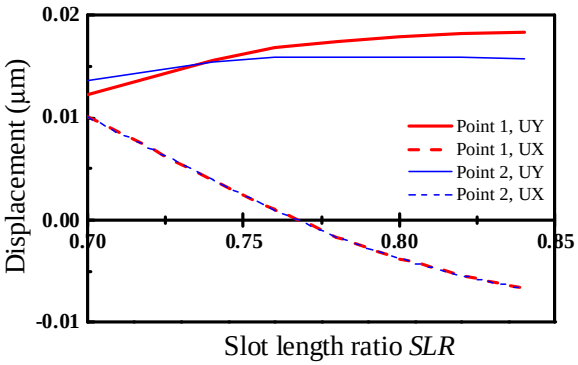

Figure 5. The displacement results versus slot dimension for the driving tip (point 1 and 2, see Fig. 3) due to the bending vibration.

The model stator and parameters for FEA are illustrated in Fig. 3. The metal body, frictional tip and PZT element sizes were fixed at 5 × 5 × 15 mm, 0.5 × 5 ×10 mm and 0.5 × 0.5 × 5 mm, respectively. The slot length ratio (*SLR* = *SL* / *VL*) and slot thickness ratio (*STR* = *ST* / *VT*) were changed.

To obtain a large mechanical output, the two vibration modes (L1 and B2 modes) should be tuned to have same resonance frequency as each other, while the displacement and direction of motion of driving tips should also be properly designed. Figure 4 shows the modal analysis simulation results for different slot size. The two vibration modes have the same resonance frequency when the *SLR* and *STR* have a certain ratio of dimensions. Despite different slot dimensions, the stator can be designed so that the two modes have the same resonance frequency by changing the *SLR* and *STR* ratio. The matched resonance frequencies (dotted line, Fig. 4) of the two modes are increased and the *STR* (thick line, Fig. 4) is decrease, when the *SLR* is increased.

The optimal slot dimension for the trial motor was determined from the displacement results of the tip by using a harmonic analysis. Figure 5 shows the displacement results along the driving tip (point 1 and 2, see Fig. 3) due to the bending vibration. If properly designed, the output tip will have a pure vertical displacement (UY) when the stator is excited by the bending mode vibration. The optimal slot ratio of *SLR* / *STR* was 0.764 / 0.26, in which the horizontal displacement (UX) of the tip was almost 0. At this condition, the resonance frequency of L1 and B2 was 142.8 kHz (see Fig. 4). The output tip displacement results excited by longitudinal mode vibration are omitted, but vertical motion (UY) was less than 2% of horizontal motion (UX) at the whole slot ratio within the range of this simulation works. Figure 6 shows the displacement angle of the driving tip, calculated from the data of Fig. 5, and also shows the representative vibration shapes with three different slot ratios to better understand the slot effects for the tip vibration. Although the slot ratios of three shapes were adjusted so that the resonance frequencies of L1 and B2 modes were matched, the tip motion was quite different with the slot shapes. Except for the optimum slot dimension, the end tips of stator have the longitudinal coupling displacement due to bending vibration.

EXPERIMENTAL SETUP

The experimental setup to measure the operation characteristics of the motor is shown in Fig. 7. The stator is supported by a pin through the centrally placed mount hole in

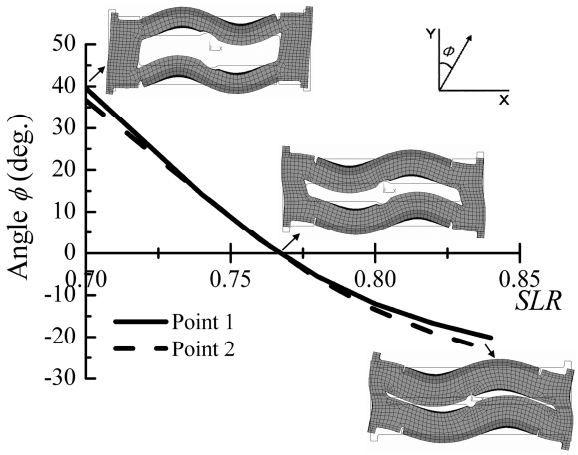

Figure 6. The displacement angle of the driving tip surface calculated from the data of Fig. 5.

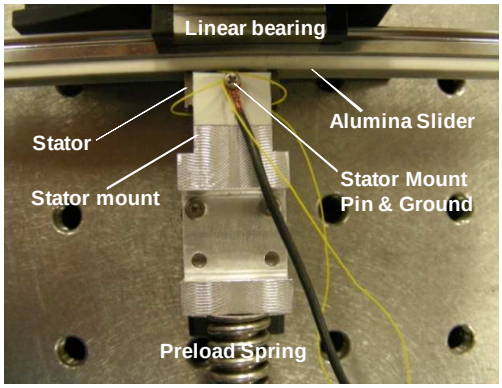

Figure 7. The experimental setup to measure the operation characteristics of the motor.

which the two vibrations have common node, providing a method to hold it without disturbing the vibrations. The stator mount pin was grounded. A 130-mm-long linear bearing, RSR-7 (THK Corporation, Japan), was used as the slider and a mirror polished alumina friction plate was bonded on the surface of the linear bearing rail. The weight of slider moving parts, including alumina plate, was 35 g. The preload between the slider and the stator was provided and changed by changing the coil spring length.

CHARACTERISTICS OF THE MOTOR

The admittance characteristics of the trial motor are measured at low voltage using an impedance analyzer (Agilent 4294A). To measure the in-phase drive admittance, all four input electrodes were connected to the *High* terminal and metal body of stator was connected to the *Low* terminal of the test fixture of the impedance analyser. However, to measure the anti-phase drive characteristics, one electrode pair (sine PZTs, Fig. 1(c)) was connected to the *High* and the other pair (cosine PZTs, Fig. 1(c)) was connected to the *Low*. The in-phase driving resonance frequency was 143.25 kHz and the anti-phase drive resonance frequency was 143.17 kHz.

The vibration velocity of the stator and driving velocity of the slider were measured by using an LDV (Graphtec AT0023+0070, Japan) [10], [11]. Figure 9 shows the two contact tip's displacement motion measured by using an LDV

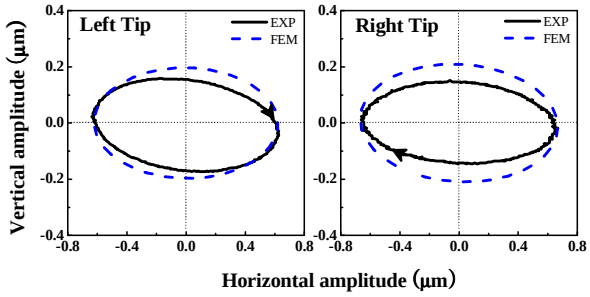

Figure 9. Left and right tip's vibration motion at 10 $V_{0\text{-}p}$ and 143.25 kHz.

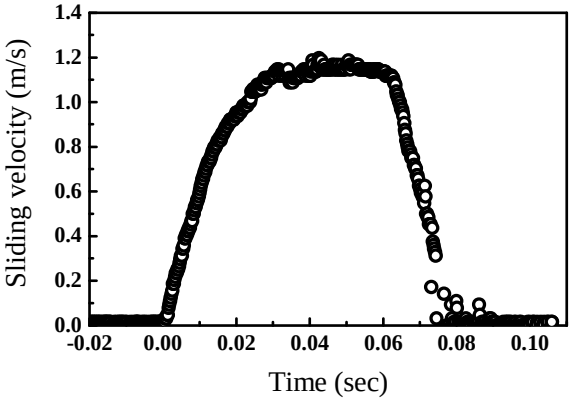

Figure 10. The measured transient response of the motor velocity with respect to time by the LDV.

at 143.25 kHz and 10 $V_{0\text{-}p}$ while driving both electrode pairs of the stator with a 90 degree phase difference.These experimental results show that the elliptical motions of the tip was well matched to the results of FEA calculations. The driving characteristics of the motor were calculated from the measured velocity of the slider with respect to time, as shown in Fig. 10. From the velocity data and the mass of the slider, the force that the motor can deliver was calculated at every point on the rise curve using the method developed by Nakamura [12]. The load characteristics of the motor were measured at the driving voltage of 70 $V_{0\text{-}p}$ and the driving frequency of 143.3 kHz, which is near the resonance frequency of the stator. The preload was changed to 2.5, 4, 10, and 15 N. The driving velocity and force curves are shown in Fig 11. In general, with an increase in the preload, the maximum sliding force also increased. We also note that while the maximum sliding force at a preload of 15 N was almost same as that with a preload of 10 N. The maximum driving force was saturated at the preload of 2.5 and 4 N, due to the limitation of friction force determined by pre-load and the frictional coefficient [4]. The maximum sliding velocity decreased slightly with an increase in preload above 4 N. At a preload of 2.5 N, however, the sliding velocity was considerably lower when compared with that of higher preloads, a result observed in other actuators [10], [13]. This low velocity could be because of the contact stiffness effect [4]. Note, as the preload is changed the resonance frequency is also changed, because the contact stiffness between the driving tip and slider directly affects the resonance frequency of the stator. At a low preload condition, the resonance frequency of the bending mode was lower than that of the longitudinal mode. However, the resonance frequency of two modes could be matched at a higher preload condition, as the mode stiffness of the bending mode is more influenced by the preload than that of the longitudinal mode [4]. For this trial linear motor, with a weight of 1.6 g, we quote a no-load velocity of 1.25 m/s at the driving voltage of 70 $V_{0\text{-}p}$ and a preload of 4 N.Figure 12 shows the velocity-force and mechanical output power characteristics of both directions at a preload of 10 N. Under this preload condition, a maximum driving velocity of 1.12 m/s and a maximum driving force of 3.4 N were achieved. The maximum mechanical output power of 1.1 W was obtained at the force of 1.63 N and the velocity of 0.68 m/s. The mechanical output power per unit weight was 688 W/kg. The mechanical output power per unit weight of the motor in this study is roughly 10 times larger than the ceramic motor by *Nanomotion* (model HR1, stator size of 3 × 7.5 × 29 mm)

In this study, a higher motor performance than previous motors was achieved by adopting titanium (Ti64) as the stator material. Titanium has a lower density and a higher transfer efficiency of ultrasonic vibration energy than PZT and phosphor bronze. In addition, by using the double driving tips attached to the position of both the highest bending and longitudinal displacement position, the maximum motor performance is increased as the driving force of the motor is transferred to the slider two times per cycle of vibration. Moreover, the bending vibration modified by the slot structure decreased the undesirable longitudinal coupling displacement of the end tips so that the elliptical motion of the two driving tips could be properly operated.

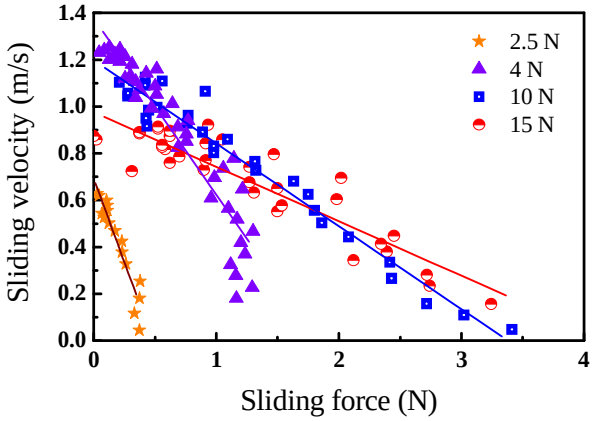

Figure 11. Load characteristics of the motor at 70 $V_{0\text{-}p}$ and 143.3 kHz.

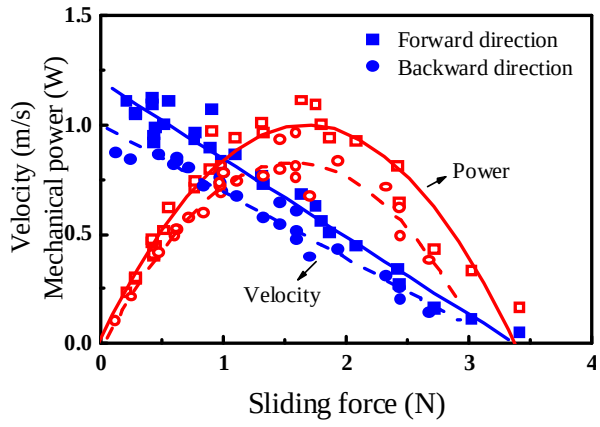

Figure 12. Load characteristics of the motor at the preload of 10 N, 70 $V_{0\text{-}p}$ and 143.3 kHz.

CONCLUSION

A novel ultrasonic micro linear motor that uses the 1st longitudinal and the 2nd bending modes, derived from a bar type stator with rectangular slot cut through the stator length was proposed, designed and tested. The slot-structure plays an important role in the motor design, which can be used not only to tune the two vibration modes to the same resonance frequency but also to decrease the undesirable longitudinal coupling displacement due to the bending vibration at the end of a stator. By using finite element analysis, the optimal slot dimension in order to improve the motion for the driving tips was determined. The trial linear motor, with a weight of 1.6 g, was given a peak no-load velocity of 1.25 m/s. Under the preload of 10 N, the maximum driving velocity of 1.12 m/s and the maximum driving force of 3.4 N were achieved. The maximum mechanical output power of 1.1 W was obtained at the force of 1.63 N and the velocity of 0.68 m/s. The mechanical output power per unit weight was 688 W/kg, which value offers the potential abilities for microrobotics and biomedical applications.

REFERENCES

1. T. Morita, M. K. Kurosawa and T. Higuchi, “Cylindrical micro ultrasonic motor utilizing bulk lead zirconate titanate (PZT),” *Jpn. J. Appl. Phys.*, vol. 38, no. 5B, pp. 3347-3350, 1998.
2. K. Uchino, “Piezoelectric actuator 2006 : Expansion from IT/robotics to ecological/energy applications,” *J Electroceram* 20, pp. 301-311, 2008.
3. W.-S. Kim, C.-H. Yun, and S.-K. Lee, “Nano positioning of a high power ultrasonic linear motor,” *Jpn. J. Appl. Phys.*, vol. 47, no. 7, pp. 5687-5692, 2008.
4. C.-H. Yun, T. Ishii, K. Nakamura, S. Ueha and K. Akashi, “A high power ultrasonic linear motor using a longitudinal and bending hybrid bolt-clamped Langevin type transducer,” *Jpn. J. Appl. Phys.*, vol. 40, no. 5B, pp. 3773-3776, 2001.
5. J. Zumeris, “Ceramic motor,” U.S. Patent 5 453 653, Sep. 26, 1995.
6. K. Spanner, “Survey of the various operating principles of ultrasonic piezomotors,” *Proceedings of the 10th International Conference on New Actuators*, 2006.
7. Y. Ming, B. Hanson, M. C. Levesley, P. G. Walker, and K. G. Watterson, “Amplitude modulation drive to rectangular-plate linear ultrasonic motors with vibrators dimensions 8 mm × 2.16 mm × 1 mm,” *IEEE Trans. Ultrason., Ferroelect., Freq. Contr.*, vol. 53, no. 12, pp. 2435–2441, 2006.
8. Y. Ming, Z. Meiling, R. C. Richardson, M. C. Levesley, P. G. Walker, K. Watterson, “Design and evaluation of linear ultrasonic motors for a cardiac compression assist device,” *Sensor and Actuators A*, vol. 119, pp. 214-220, 2005.
9. C. Lu, T. Xie, T. Zhou, and Y. Chen, “Study of a new type linear ultrasonic motor with double-driving feet,” *Ultrasonics*, vol. 44, pp. 585-589, 2006.
10. J. Friend, Y. Gouda, K. Nakamura, and S. Ueha, “A simple bidirectional linear microactuator for nanopositioning—the “Baltan” microactuator,” *IEEE Trans. Ultrason., Ferroelect., Freq. Contr.*, vol. 53, no. 6, pp. 1160–1168, 2006.
11. J. Friend, K. Nakamura, and S. Ueha, “A traveling-wave, modified ring linear piezoelectric microactuator with enclosed piezoelectric elements - the "scream" actuator,” *IEEE Trans. Ultrason., Ferroelect., Freq. Contr.*, vol. 52, no. 8, pp. 1343–1353, 2005.
12. K. Nakamura, M. Kurosawa, H. Kurebayashi, and S. Ueha, “An estimation of load characteristics of an ultrasonic motor by measuring transient responses,” *IEEE Trans. Ultrason., Ferroelect.,Freq. Contr.*, vol. 38, no. 5, pp. 481–485, 1991.
13. J. Friend, J. Satonobu, K. Nakamura, S. Ueha, and D. S. Stutts, “A single-element tuning fork piezoelectric linear actuator,” *IEEE Trans. Ultrason., Ferroelect., Freq. Contr.*, vol. 50, no. 2, pp. 179–186, 2003.